ELSEVIER

Journal of Structural Geology 26 (2004) 1521–1529

JOURNAL OF STRUCTURAL GEOLOGY

www.elsevier.com/locate/jsg

Calcite twin morphology: a low-temperature deformation geothermometer

David A. Ferrill[a,*], Alan P. Morris[b], Mark A. Evans[c], Martin Burkhard[d], Richard H. Groshong Jr.[e], Charles M. Onasch[f]

[a]*Center for Nuclear Waste Regulatory Analyses, Southwest Research Institute, 6220 Culebra Rd., San Antonio, TX 78238-5166, USA*
[b]*Department of Earth and Environmental Science, University of Texas at San Antonio, San Antonio, TX 78249, USA*
[c]*Department of Geology and Planetary Science, University of Pittsburgh, Pittsburgh, PA 15260, USA*
[d]*Institut de Géologie, rue E. Argand 11, CH-2000 Neuchâtel, Switzerland*
[e]*Department of Geology and Geography, University of Alabama, Tuscaloosa, AL 35487, USA*
[f]*Department of Geology, Bowling Green State University, Bowling Green, OH 43403, USA*

Received 13 November 2002; received in revised form 21 October 2003; accepted 6 November 2003

Available online 12 February 2004

Abstract

Twinning of the e-plane is the dominant crystal–plastic deformation mechanism in calcite deformed below about 400 °C. Calcite in a twin domain has a different crystallographic orientation from the host calcite grain. So-called thin twins appear as thin black lines when viewed parallel to the twin plane at 200–320 × magnification under a petrographic microscope. Thick twins viewed in the same way have a microscopically visible width of twinned material between black lines. Calcite e-twin width and morphology has been correlated with temperature of deformation in naturally deformed coarse-grained calcite. In this paper, we present a compilation and analysis of data from limestones of the frontal Alps (France and Switzerland) and the Appalachian Valley and Ridge and Plateau provinces (eastern United States) to document this temperature dependence. Mean calcite twin width correlates directly with temperature of deformation such that thin twins dominate below 170 °C and thick twins dominate above 200 °C. Above 250 °C dynamic recrystallization is an important deformation mechanism in calcite. Mean twin intensity (twin planes/mm) correlates negatively with temperature, and a cross plot of twin intensity with twin width can yield information about both strain and temperature of deformation. These relationships provide a deformation geothermometer for rocks that might otherwise yield little or no paleotemperature data.

Keywords: Calcite; Twinning; Deformation; Geothermometry; Alps; Appalachians

1. Introduction

Mechanical e-twinning of calcite is the dominant crystal–plastic deformation mechanism in coarse-grained limestone and marble deformed at temperatures below about 400 °C (Turner, 1953; Carter and Raleigh, 1969; Groshong, 1988). Twins in calcite deformed at temperatures below 170 °C are typically thin, appearing only as thin black lines under the optical microscope (Fig. 1). Thickness is measured as the perpendicular distance between boundaries with the twin rotated to vertical on a universal stage. Such twins are most commonly less than one micron (1 micron = 0.001 mm) thick. In limestone and marble deformation experiments performed at room temperature (about 25 °C), increasing calcite twin strain results in development of new thin twins; therefore, the twin intensity (#/mm) increases (Turner and Ch'ih, 1951; Turner, 1953; Groshong, 1974; Ferrill, 1998). Experimental deformation of calcite at temperatures of 300 °C and above produces twins that have a width of twinned material that is distinguishable under the microscope, and individual twins may exceed 5 microns in width. Such thick twins also occur in naturally deformed rocks and are commonly lensoid in shape, tapering towards the grain boundaries (Heard, 1963; Schmid et al., 1980; Rowe and Rutter, 1990). Groshong et al. (1984a) identified a transition in twin morphology associated with increasing temperature of deformation in the Helvetic Alps. Twin morphologies define a spectrum that corresponds to increasing temperature from thin twins at very low temperature to straight thick twins, to bent thick twins, and finally to recrystallization at grain boundaries (Fig. 1).

Working definitions of thin versus thick calcite twins are

* Corresponding author. Tel.: +1-210-522-6082; fax: +1-210-522-5155.
E-mail address: dferrill@swri.edu (D.A. Ferrill).

0191-8141/$ - see front matter © 2004 Elsevier Ltd. All rights reserved.
doi:10.1016/j.jsg.2003.11.028

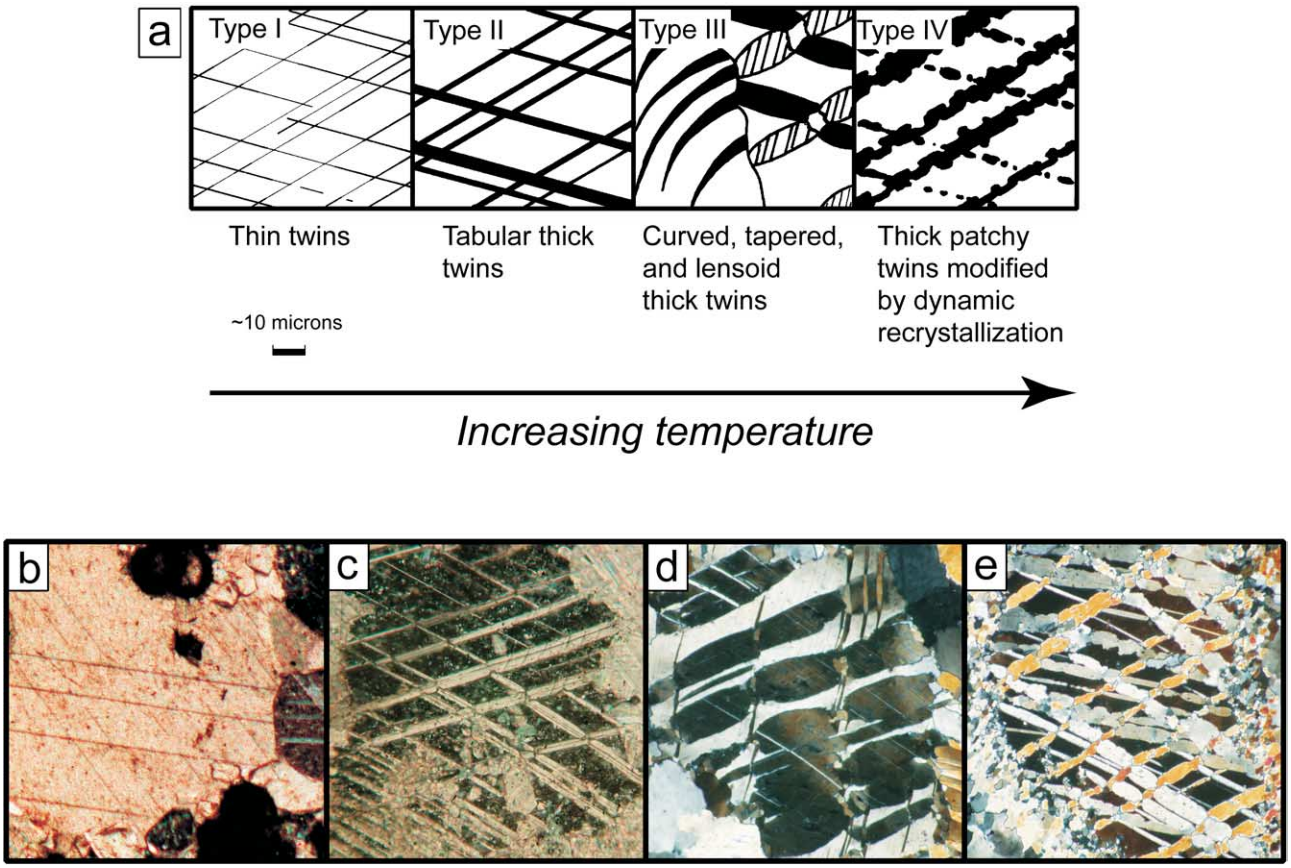

Fig. 1. (a) Schematic illustration of the influence of temperature on deformation by calcite twinning (after Burkhard, 1993). Photomicrograph examples of different twin types (all in cross-polarized light). (b) Type I twins from the northern Subalpine Chain, France (sample 87-25d; Ferrill, 1991). Width of the photomicrograph is 0.68 mm. (c) Type II twins from the North Mountain thrust sheet (sample W91) in the Great Valley, Central Appalachian Valley and Ridge Province (Evans and Dunne, 1991). Note that thin twins are locally developed within thick twins. Width of the photomicrograph is 0.22 mm. (d) Type III twins from the Ardon thrust slice of the Diablerets nappe (sample 691.1) in the Helvetic Alps (Burkhard, 1990). Width of the photomicrograph is 0.14 mm. (e) Type IV twins from the Doldenhorn nappe (sample 199.3) in the Helvetic Alps (Burkhard, 1990). Width of the photomicrograph is 0.14 mm. Photomicrographs (d) and (e) are from ultra-thin sections (thickness of approximately 5 microns or less).

given by Groshong (1974). In crossed polarized light, both thin and thick twins oriented at a high angle to the microscope axis produce obvious parallel color fringes. When the twins are rotated to parallel the microscope axis, the color fringes disappear and what is seen is either a finite width of twinned material (thick twin) or a black line of measurable width (thin twin). Conel (1962) showed that the color bands are interference fringes predictable from the wave properties of light acting on the twinned material. Fractures and open cleavages do not show color fringes and so are easily distinguished from twins using a universal stage (U-stage) microscope. Thin twins appear in thin sections as black lines when observed using a universal stage at 200–320 × magnification. Spang et al. (1974) demonstrated using scanning electron microscope observations that thin twins do, in fact, include discernible amounts of twinned material. The thin–twin black line width includes a combination of twinned material and the optical effects due to the twin boundaries. Using measured and calculated strains from experimentally deformed twinned calcite in limestone, Groshong (1974) determined that approximately 50% of the black line width represents twinned calcite (also see Groshong et al., 1984b). Thick calcite twins can be resolved optically from the untwinned host. Under cross-polarized light, the calcite within a thick twin can be seen to go to extinction in a different position from that in the untwinned host calcite. Widths of thick twins measured as the distance between the inner edges of the visible twin boundaries range from approximately 1 to >10 microns. The calculations and graphical techniques presented in this paper use data that were rigorously gathered using the calcite strain gauge technique (Groshong, 1974; Evans and Groshong, 1994). For the analysis presented here, it is important that twin intensities and twin widths were measured, not assumed. In addition, for consistency, we have used data collected from coarse-grained limestones (grainstones and packstones), and analyzed twinning in coarse fossil fragments and cements rather than vein calcite. In general, twin analysis was performed on grains 50–500 microns in diameter.

The relationship between calcite twin width and metamorphic grade has been observed in naturally deformed limestones from the Central Appalachians (compare Groshong (1972, 1975) and Spang and Groshong (1981) with Evans and Dunne (1991) and Ferrill (1991)), the Helvetic Alps (Groshong et al., 1984a; Burkhard, 1986), the Prealps (Mosar, 1989), and the northern Subalpine Chain (Ferrill, 1991; Ferrill and Groshong, 1993). The consistency of this relationship and its ease of application make it a useful geothermometer. The calcite twin data and metamorphic data from these studies are here combined with additional twin and metamorphic data from the Alps and Appalachians to improve calibration of this deformation geothermometer. This paper builds on the work of Ferrill (1991) and Burkhard (1993), and provides the quantitative basis for estimation of deformation temperature using calcite twin width, intensity, and strain data. When used with additional microstructural data to interpret relative timing of twinning, calcite deformation geothermometry could be applied to such problems as interpreting geothermal gradients and isotherm migration, and interpreting the relative timing of hydrocarbon trap formation with respect to kerogen maturation.

2. Calcite twin strain, twin geometry and recrystallization methods

2.1. Calcite twinning

Calcite twin strain in coarse-grained limestones is measured using the calcite strain gauge technique of Groshong (1972, 1974) and Evans and Groshong (1994). Careful preparation of thin sections is required so that grains are not fractured or twinned during sample preparation. For each twin set measured, the average twin width, number of twins, grain width normal to twins, and the orientations of the c-axis and the e-twin plane are measured using a U-stage (Evans and Groshong, 1994). Widths of thin and thick twins are measured separately. Groshong (1974) showed that a total of 50 twin sets, measured for each sample on two orthogonal planes, yield statistically the same result as a total of 150 measurements. The principal strains (e_1, e_2, and e_3; expressed in % as + or − changes in length) and their orientations are calculated and output along with values of negative expected value (twin sets with sense of shear inconsistent with calculated strain tensor) and error. There is always natural variation around a population mean and there may be operator error. Groshong (1974) showed experimentally that eliminating the twin sets with the largest deviations from the mean (approximately 20%, often referred to as 'largest deviations removed' or LDR) gives a better match between measured and experimental strain magnitudes. This cleaning procedure is also typically applied to natural samples. The square root of the second invariant of strain ($\sqrt{J_2}$%) is here used as a measure of the total distortion by twinning (Jaeger and Cook, 1979). J_2 is calculated from the three principal strains as follows: $J_2 = -(e_2e_3 + e_3e_1 + e_1e_2)$, where e_1, e_2, and e_3 are expressed as %.

The 'mean twin width' for a sample is determined by first calculating the average twin width for each twin set (twin-set average) and then averaging the twin-set averages for the sample. Each twin set average is calculated by summing the width of twinned material in a twin set, including both thick and thin twins, and dividing this by the total number of twins in the set. In the present study, the standard twin-width sample average only includes twin sets used in the final twin strain calculation and does not include sets removed during cleaning.

The twin intensity (twin planes/mm) for each twin set is calculated by dividing the number of twins in a set (including both thick and thin twins) by the width of the host grain measured perpendicular to the twins. The 'mean twin intensity' for a sample is calculated by averaging the twin-set averages for all twin sets measured in the sample. As with the twin width data, the mean twin intensity values only include twin sets used in the final twin strain calculation.

2.2. Results of calcite twin width and intensity analysis

The calcite twin data presented here are in part from previously published studies, but also include new data (e.g. mean twin width and intensity) (Table 1). The metamorphic information for the studies includes mean vitrinite reflectance (Ferrill, 1991; Ferrill and Groshong, 1993), illite crystallinity (Groshong et al., 1984a; Ferrill, 1991; Xu, 1993; Xu et al., 1993), conodont color alteration index (Evans and Dunne, 1991; Smart et al., 1997; Spraggins and Dunne, 2002), maximum depth of burial interpretations (Smart et al., 1997; Spraggins and Dunne, 2002), fluid inclusion microthermometric data (M.A. Evans unpublished data for Smart et al. (1997) study area), and deformation mechanism maps (Evans and Dunne, 1991). In each case, the maximum metamorphic temperatures have been estimated to provide a basis for thermal comparison from study to study. Although crystal–plastic deformation can occur at any time during burial and exhumation, we have focused this analysis on examples where crystal–plastic deformation was coeval with maximum burial. Table 1 gives a tabulation of previously unpublished data used in graphs plotted in this paper, and the necessary supporting data that are typical for calcite strain gauge analyses.

2.3. Alps

The Alpine foreland fold–thrust belts consist of Mesozoic and Tertiary sedimentary strata deformed during the Cretaceous through Quaternary Alpine orogeny. The deformed strata are largely carbonate and fine-grained clastic rocks with a relatively small proportion of coarse

Table 1
Tabulation of calcite twin data that have not been published previously. All data were cleaned by removing the ~20% of twin sets with largest deviations (LDR), following the procedure of Groshong (1974)

Sample	Twin sets rem.	Twin sets	Principal strains %			Width (microns)	Intensity (#/mm)	$\sqrt{J_2}$ (%)	Max. T (°C)
			e_1	e_2	e_3				
Eastern Helvetic Alps, Switzerland (Groshong et al., 1984a)									
AD 80-23	20	86	0.59	−0.32	−0.54	0.53	26.8	0.58	70–180
AD 80-16	7	28	2.07	−0.18	−1.90	1.16	46.4	1.99	250–300
AD 80-15	17	70	1.38	0.62	−2.00	0.64	35.2	1.77	160–190
AD 80-25	24	94	2.23	0.09	−3.14	0.69	55.6	2.66	70–180
AD 80-20	18	71	2.51	−0.69	−1.81	1.35	71.1	2.24	300–350
AD 80-24	28	114	3.00	−0.07	−2.93	0.68	64.4	2.97	70–180
AD 80-19	15	66	3.58	−0.63	−2.96	3.92	22.8	3.31	250–300
AD 80-12	20	81	4.08	−1.32	−2.76	1.20	51.0	3.61	170–250
AD 80-21	14	55	3.79	0.88	−4.67	0.96	88.3	4.30	70–180
AD 80-17	13	50	5.16	0.09	−5.30	2.78	27.6	5.23	250–300
AD 80-11	20	78	3.87	1.87	−5.74	2.17	33.8	5.07	170–250
AD 80-13	17	67	6.07	3.22	−9.29	3.62	55.5	8.17	170–250
AD 80-14	16	65	6.88	4.59	−11.47	0.60	26.2	10.00	170–250
Western Great Valley, Virginia (Evans and Dunne (1991) and unpublished data)									
T14	10	40	0.80	0.21	−0.82	0.87	18.12	0.81	250–350
H81	10	40	1.14	0.08	−1.21	1.22	13.26	1.18	250–350
S44	10	40	1.14	0.66	−1.80	0.96	18.81	1.58	250–350
T31	10	41	1.50	0.48	−1.97	1.88	15.47	1.78	250–350
H84	10	41	2.42	−0.66	−1.77	1.79	13.49	2.17	250–350
M71	10	41	2.12	0.25	−2.37	1.70	16.96	2.26	250–350
B42	10	40	2.00	0.46	−2.47	2.33	16.58	2.27	250–350
T13	10	41	2.58	−0.76	−1.82	1.66	19.82	2.30	250–350
C72	10	41	2.91	−0.54	−2.37	1.72	24.02	2.68	250–350
T64	10	41	2.07	1.07	−3.15	1.82	26.46	2.77	250–350
W81	10	40	2.79	0.36	−3.15	2.20	20.56	2.99	250–350
B33	10	41	2.96	0.46	−3.42	2.53	19.22	3.21	250–350
H31	11	40	2.76	0.76	−3.52	1.97	25.73	3.21	250–350
W92	10	41	3.38	−0.16	−3.23	1.93	20.43	3.31	250–350
N51	10	42	3.78	−1.28	−2.50	2.44	20.64	3.33	250–350
P71	10	40	3.85	0.04	−3.89	2.41	20.60	3.87	250–350
M31	10	40	3.46	1.07	−4.53	2.62	20.40	4.10	250–350
S12	11	42	4.77	−0.61	−4.16	2.47	27.32	4.50	250–350
W82	10	40	5.87	−0.54	−5.34	2.49	36.41	5.62	250–350
T51	11	40	5.89	−0.48	−5.41	2.71	22.65	5.67	250–350
B51	10	40	11.40	−4.74	−6.66	4.06	21.19	9.92	250–350
Massanutten Synclinorium, Virginia (Onasch, unpublished data)									
MS102	10	40	2.29	−0.55	−1.74	1.17	40.30	2.07	~200
MS53	4	16	2.02	0.95	−2.97	1.11	28.63	2.63	~200
MS90	10	40	2.15	1.15	−3.30	1.37	38.56	2.90	~200
MS103	10	40	2.84	0.70	−3.54	1.13	46.82	3.25	~200
MS106	10	40	2.78	1.23	−4.01	1.86	37.21	3.56	~200
MS57	10	40	4.53	−0.69	−3.83	2.08	34.83	4.22	~200
MS94	8	32	4.01	1.67	−5.68	1.77	39.99	5.06	~200
MS105	10	40	4.17	1.8	−5.97	1.56	46.15	5.30	~200
MS101	10	40	4.69	1.13	−5.83	1.66	43.69	5.35	~200
MS96	10	40	6.71	−1.35	−5.36	2.67	35.36	6.15	~200
MS182	10	40	7.36	2.15	−9.51	1.89	49.39	8.64	~200
MS99	10	40	8.78	−0.18	−8.59	3.11	28.81	8.69	~200
MS92	10	40	7.25	3.32	−10.56	2.32	64.02	9.36	~200

Note: Temperature estimates for Massanutten Synclinorium samples from illite crystallinity of underlying Martinsburg Formation.

clastic units. The foreland fold–thrust belts of the Swiss and French Alps consist of the Helvetic Alps and Subalpine chains in Switzerland and France, respectively, on the hinterland side (east and southeast) of the Molasse basin, and the Jura on the foreland side (west and northwest) of the Molasse basin. Structurally overlying the Helvetic Alps and Subalpine chains are klippen of far-traveled thrust sheets above the Pennine thrust, which are known as the Prealps. The degree of low-grade metamorphism generally increases from the foreland to the hinterland across the Helvetic Alps

and Subalpine chains. Strata of the same age, composition, and sedimentary fabric have been sampled around and across the foreland fold–thrust belts and show a strong relationship between peak metamorphism and calcite twin morphology, and presence or absence of dynamic recrystallization in coarse calcite. These relationships have been observed independently in the eastern Helvetic Alps (Groshong et al., 1984a), the western Helvetic Alps (Burkhard, 1986, 1993), the northern Subalpine chains (Ferrill, 1991; Ferrill and Groshong, 1993), and in the Prealps (Mosar, 1988; 1989).

2.4. Appalachians

The Appalachian foreland fold–thrust belt consists of Cambrian through Carboniferous sedimentary strata deformed during the late Paleozoic Alleghenian orogeny. The deformed strata consist of a thick sequence of Cambrian and Ordovician carbonate rocks, overlain by thinner Ordovician to Carboniferous carbonate and clastic strata. The Appalachian foreland fold–thrust belt consists of two provinces: the Appalachian Plateau Province on the foreland side (Smart et al., 1997; Spraggins and Dunne, 2002), and the Valley and Ridge Province on the hinterland side. The Valley and Ridge Province of the Central Appalachians (West Virginia, Pennsylvania, Maryland, Virginia) is divided into two sub provinces, separated by the North Mountain thrust. East of the North Mountain thrust is the Great Valley, which primarily consists of Cambro–Ordovician carbonate rocks at the surface (Evans and Dunne, 1991). The Massanutten synclinorium is a large syncline within the Great Valley sub-province that exposes strata as young as Devonian in age (Xu, 1993; Xu et al., 1993). West of the North Mountain thrust, and east of the Appalachian structural front is the western Valley and Ridge Province, which consists of Ordovician through Carboniferous strata at the surface. In the present compilation of calcite microstructural data from the Appalachians (Evans and Dunne, 1991; Smart et al., 1997; Xu, 1993; Xu et al., 1993), the bulk of the data come from the Central Appalachians, although one data set comes from the transition between the central and southern Appalachians (Spraggins and Dunne, 2002). In the Central Appalachians, the Cambro–Ordovician carbonates experienced considerably higher temperatures than the carbonate strata exposed in the western Valley and Ridge.

2.5. Twin morphology, temperature of deformation, and strain

Calcite twin data from both the Alps and the Appalachians, spanning a wide spectrum of depositional ages and timing of deformation, exhibit a dependence of twin width on temperature of deformation and strain (Fig. 2a) (Ferrill, 1991). Fig. 2a also illustrates the relationship between twin strain and mean twin width: higher strains are associated with wider twins (Ferrill, 1991). Twin intensities vary inversely with temperature. Calcite deformed at higher temperatures exhibits a narrow range of low twin intensities when compared with calcite deformed at low temperatures (Fig. 2b). There is a strong clustering of data with respect to temperature, and domains of data characterized by deformation at maximum temperatures <170, 170–200, and >200 °C can be differentiated on graphs comparing mean twin width, mean twin intensity, and twin strain (see dashed lines in Fig. 2a–c). At higher temperatures, calcite develops thick twins and low twin intensities. At lower temperatures, calcite develops thin twins and high twin intensities (Fig. 2c). Calcite twin strain can accumulate by increasing the number of twins (increasing mean twin intensity), increasing the size of twins (increasing the mean twin width), or both. The product of mean twin width and mean twin intensity yields the ratio of twinned to untwinned crystal. This ratio is directly proportional to the amount of shear strain experienced by the sample and is relatively insensitive to the temperature of deformation (Fig. 2d). Groshong (1972) derives an equation for the relationship between shear strain accommodated by a calcite twin set, the grain size, and the twin width (Eq. 1 in Groshong, 1972). This equation can be rearranged to express shear strain accommodated by a twin set in terms of twin intensity and twin width:

$$\gamma = Tt2\tan\left(\frac{\alpha}{2}\right) \tag{1}$$

where γ = shear strain, T = twin intensity, t = twin width, and α = angle of rotation of the grain edge from the untwinned to the twinned position, and is equal to 38°17′ (38.28°; Handin and Griggs, 1951; Groshong, 1972). Calcite twin sets for each sample are measured for a variety of arbitrary orientations, each representing a shear strain value for that direction within the strain tensor recorded by the calcite twinning mechanism. These results are arithmetically averaged to obtain the reported mean twin intensity and mean twin width values. Because twin width and intensity together determine the amount of shear strain that is accommodated by twinning, a given shear strain can be accommodated by sets of twin width and intensity values as described by Groshong (1972). Therefore, contours of equal strain in terms of twin intensity and twin width should approximate the form of Groshong's Eq. (1) (Groshong, 1972). Fig. 3 shows this to be the case.

2.6. Dynamic recrystallization

Dynamic recrystallization in calcite rocks tends to occur along grain boundaries and along twins, migrating inward from the grain boundary (Groshong, 1988; Burkhard, 1993) and forming serrated (Hobbs et al., 1976, p. 115) or jigsaw-puzzle-like grain boundaries (Groshong, 1988, p. 1331; Schmid et al., 1980; Schmid, 1982, fig. 5). Continued dynamic recrystallization leads to mortar texture (Spry,

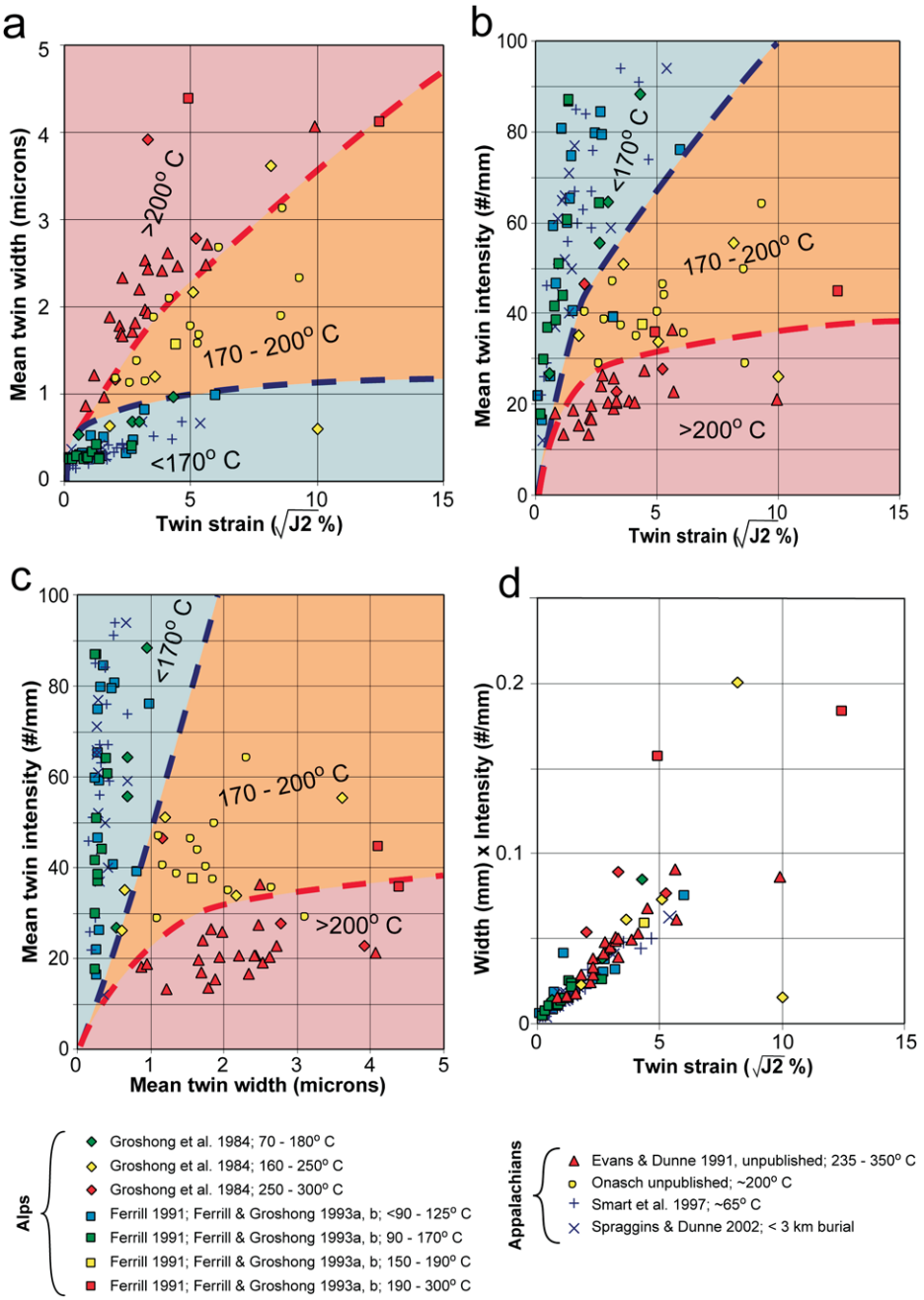

Fig. 2. Graphs of twin parameters from the Alps and Appalachians color-coded according to interpreted deformation temperature from peak burial or metamorphic indicators. (a) Mean twin width versus twin strain, (b) mean twin intensity versus twin strain, (c) mean twin intensity versus mean twin width, (d) product of mean twin width and mean twin intensity (ratio of twinned to untwinned crystal) versus twin strain. Plots include data from Table 1; Ferrill (1991; LDR data), Spraggins and Dunne (2002; uncleaned data), and Smart et al. (1997; uncleaned data). Unpublished fluid inclusion microthermometric data of M.A. Evans were used to constrain ~65 °C temperature for sample locations from Smart et al. (1997) and >235 °C constraint on data from Evans and Dunne (1991). Dashed lines separate domains of data characterized by deformation at temperatures of <170, 170–200, and >200 °C as labeled.

1969, Pl. XXVIII) or core-mantle structure (Schmid et al., 1980) and recrystallization of twins progressing in from the grain boundaries. In large grains (especially monomineralic vein calcite), and at high strain rates, dynamic recrystallization of deformed calcite may be activated by high dislocation densities rather than by elevated temperatures (Kennedy and White, 2001). Thus, dynamic recrystallization is both grain-size and temperature dependent, which under certain conditions may begin at temperatures lower than 250 °C. In this study we use only results from non-vein calcite, and from samples outside localized fault zones. Recrystallization can entirely destroy primary rock textures as seen in the Lochseiten mylonite along the Glarus thrust, Switzerland (Schmid et al., 1980, figs. 14–16). These textures are characterized by large grains surrounded and invaded by small subgrains. Onset of dynamic recrystallization has

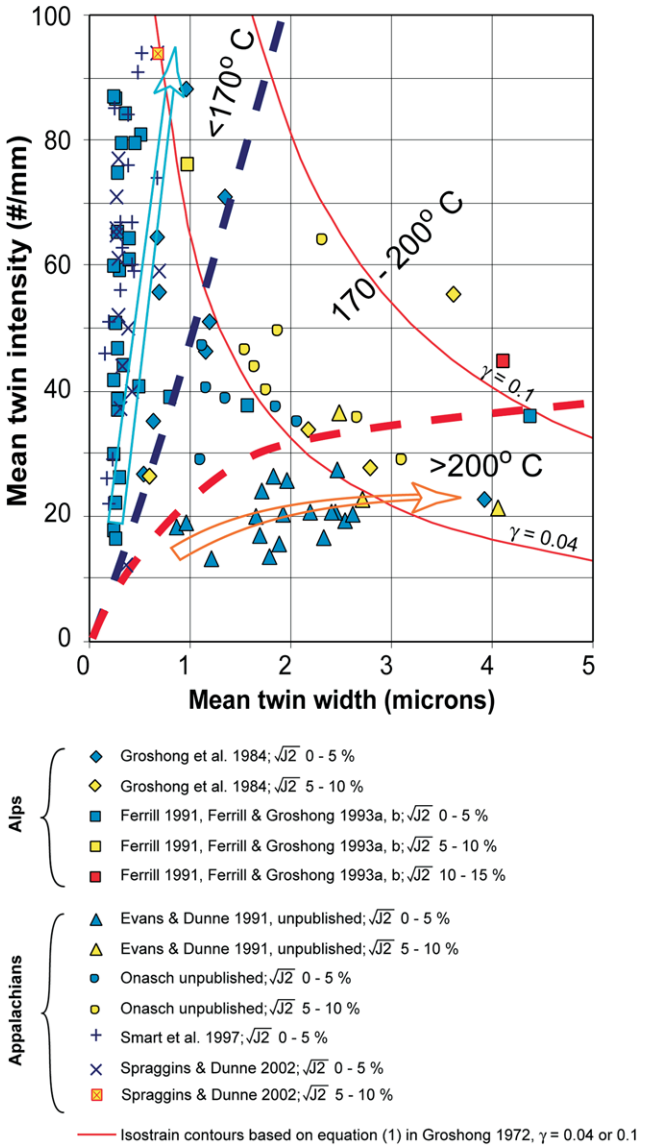

Fig. 3. Graph of mean twin intensity versus mean twin width with data points colored according to twin strain. Orange and blue arrows illustrate paths of increasing strain for temperatures >200 and <170 °C, respectively. Red lines are isostrain contours derived from Eq. (1) in Groshong (1972).

been referred to as the tectonite front (Groshong, 1988), and Burkhard (1993) correlates this onset with the boundary between type III and type IV twinning (Fig. 1). In naturally deformed coarse-grained calcite rocks in the Helvetic Alps, Prealps, Subalpine Chains, and the Appalachians, onset of dynamic recrystallization tends to coincide with a peak metamorphic temperature in the range of 250–350 °C. Temperatures for onset of dynamic recrystallization of 250 °C were reported from the eastern and western Helvetic Alps of Switzerland (Groshong et al., 1984a; Burkhard, 1993) and the northern Subalpine Chain of France (Ferrill and Groshong, 1993), 300 °C from the Prealps Medianes of Switzerland (Mosar, 1989), and 350 °C from the Central Appalachians of the eastern USA (Evans and Dunne, 1991).

3. Discussion

Calcite twin width and temperature of deformation are positively correlated, and distinct changes in dominant twin morphology occur between 170 and 200 °C (Fig. 2a). Deformation microstructures in calcite are dominated by thin twins below 170 °C and thick twins above 200 °C. Calcite deformed at temperatures below 170 °C accumulates crystal plastic strain by the formation of new thin twins rather than by twin enlargement or the formation of thick twins. At higher temperatures, a larger proportion of thicker twins form to accommodate increased strain, and thermally activated twin boundary migration further increases the mean observed twin width. Above 200 °C most twins are large enough to be classified as thick twins, and mean twin widths are commensurately larger. Strain accumulation at temperatures above 200 °C is accomplished by the formation of thick twins and the enlargement of existing twins rather than by thin twin formation. Twin intensities in rocks deformed above 200 °C rarely exceed 40 per mm (Fig. 2b).

Twin width and twin intensity are necessarily inversely correlated in rocks that have experienced similar amounts of shear strain (Fig. 3). This inverse relationship is illustrated by the fact that samples deformed at temperatures <170 °C have small mean twin widths (≤1 micron) over a wide range of strain magnitudes ($\sqrt{J_2}\% = 0–5\%$) (Fig. 2a), whereas those deformed at temperatures >200 °C exhibit a narrow range of twin intensities (0–40 per mm) over a wide range of strain magnitudes ($\sqrt{J_2}\% = 0–6\%$). In general, rocks deforming at low temperatures will accumulate calcite twin strain (not necessarily bulk strain) along paths similar to the blue arrow in Fig. 3. Strain accumulation occurs primarily by the formation of new thin twins and the concomitant increase in twin intensity. Rocks deforming at high temperatures (>200 °C) will accumulate calcite twin strain along paths similar to the orange arrow in Fig. 3.

The largest twin strain magnitudes are seen in rocks deformed at higher temperatures. Mechanical twinning of calcite, however, only records the crystal–plastic component of the total rock strain. Other mechanisms in carbonate rocks, particularly pressure solution and brittle faulting and fracturing, also contribute to the bulk strain. The inverse relationship between pressure solution and crystal–plastic mechanisms of deformation is well documented (e.g. Rutter, 1976), and it is likely that the correlation between twin strain and temperature results from temperature weakening of calcite and the increasing effectiveness of crystal–plastic mechanisms over intercrystalline and transgranular mechanisms at higher temperatures (Donath, 1970; Donath et al., 1971; Ferrill and Groshong, 1993).

Thermal history can have a significant effect on the observed deformation microstructures. For example, twinning at >200 °C during increasing temperature (to 300 °C) may be manifest by thick twins, grain boundary recrystallization, and recrystallization that has advanced inward from

the grain boundaries. In contrast, twinning occurring at >200 °C followed by decreasing temperature would likely exhibit thick twins, no grain boundary recrystallization, and a greater abundance of thin twins, some in the same set as the thick twins and perhaps others cutting the thick twins.

The results presented here provide a quantitative approach for estimating deformation temperature from coarse-grained limestones—rocks that typically lack alternative measures of deformation temperatures or maximum temperatures. Additional investigation of calcite deformation in coarse-grained limestones could further refine this approach to geothermomentry in the temperature range from 25 to 250 °C, and may include: (i) analysis of twin width, intensity, and strain in *experimentally* deformed rocks focusing on deformation in the temperature range from 25 to 250 °C, (ii) exploration of the crystal-lattice scale controls on twin initiation versus twin widening (thin versus thick twinning), (iii) detailed recording of each twin (e.g. width and spacing) used in calcite strain gauge analysis and characterization of the twin width distribution in experimentally and naturally twinned calcite in coarse-grained limestones, and (v) additional exploration of the effects of grain size, confining pressure, and differential stress on twin strain in relatively low temperature deformation of limestone.

4. Summary and conclusions

Our compilation of data from limestones from the Alps (France and Switzerland), and the Appalachians (eastern United States) documents the deformation–temperature dependence of calcite twin geometry. Mean calcite twin width correlates directly with temperature of deformation such that thin twins dominate below 170 °C and thick twins dominate above 200 °C. Above 250 °C dynamic recrystallization is an important deformation mechanism in calcite. Mean twin intensity (twin planes/mm) correlates negatively with temperature, and a cross plot of twin intensity with twin width can yield information about both strain and temperature of deformation. These relationships provide a deformation geothermometer for rocks that might otherwise provide little or no paleotemperature data.

Acknowledgements

We thank John Mosar and Ted Apotria for their collaboration and many discussions during the early stages of this project. We thank Bill Dunne for useful discussions of data from the Appalachian Plateau. Critical reviews by Nathan Franklin, Pat Mackin, Giancarlo Molli, Bernd Leiss, and Tom Blenkinsop greatly improved this manuscript. Much of this work was presented at the 1992 Penrose Conference titled “Application of Strains from Microstructures to Mountain Belts”.

References

Burkhard, M., 1986. Déformation des calcaires de l’Helvétique de la Suisse occidentale (Phénomènes, mécanismes et interprétations tectoniques). Revue de Geologie dynamique et de Géographie Physique 27, 281–301.

Burkhard, M., 1990. Ductile deformation mechanisms in micritic limestones naturally deformed at low temperatures (150–350 °C). In: Knipe, R.J., Rutter, E.H. (Eds.), Deformation Mechanisms, Rheology and Tectonics. Special Publication of the Geological Society of London 54, pp. 241–257.

Burkhard, M., 1993. Calcite twins, their geometry, appearance and significance as stress–strain markers and indicators of tectonic regime: a review. Journal of Structural Geology 15, 351–368.

Carter, N.L., Raleigh, C.B., 1969. Principal stress directions from plastic flow in crystals. Bulletin of the Geological Society of America 80, 1231–1264.

Conel, J.E., 1962. Studies of the development of fabrics in some naturally deformed limestones. Ph.D. dissertation, California Institute of Technology, Pasadena.

Donath, F.A., 1970. Some information squeezed out of rock. American Scientist 58, 54–72.

Donath, F.A., Faill, R.T., Tobin, D.G., 1971. Deformation mode fields in experimentally deformed rock. Geological Society of America Bulletin 82, 1441–1462.

Evans, M.A., Dunne, W.M., 1991. Strain factorization and partitioning in the North Mountain thrust sheet, central Appalachians, USA. Journal of Structural Geology 13, 21–35.

Evans, M.A., Groshong, R.H. Jr, 1994. A computer program for the calcite strain gauge technique. Journal of Structural Geology 16, 277–281.

Ferrill, D.A., 1991. Calcite twin widths and intensities as metamorphic indicators in natural low-temperature deformation of limestone. Journal of Structural Geology 13, 667–675.

Ferrill, D.A., 1998. Critical re-evaluation of differential stress estimates for calcite twins in coarse-grained limestone. Tectonophysics 285, 77–86.

Ferrill, D.A., Groshong, R.H. Jr, 1993. Deformation conditions in the northern Subalpine Chain, France, estimated from deformation modes in coarse-grained limestone. Journal of Structural Geology 15, 995–1006.

Groshong, R.H. Jr, 1972. Strain calculated from twinning in calcite. Bulletin of the Geological Society of America 82, 2025–2038.

Groshong, R.H. Jr, 1974. Experimental test of least-squares strain gage calculation using twinned calcite. Bulletin of the Geological Society of America 58, 1855–1864.

Groshong, R.H. Jr, 1975. Strain, fractures, and pressure solution in natural single-layer folds. Bulletin of the Geological Society of America 86, 1363–1376.

Groshong, R.H. Jr, 1988. Low-temperature deformation mechanisms and their interpretation. Bulletin of the Geological Society of America 100, 1329–1360.

Groshong, R.H. Jr, Pfiffner, O.A., Pringle, L.R., 1984a. Strain partitioning in the Helvetic thrust belt of eastern Switzerland from the leading edge to the internal zone. Journal of Structural Geology 6, 5–18.

Groshong, R.H. Jr, Teufel, L.W., Gasteiger, C., 1984b. Precision and accuracy of the calcite strain-gage technique. Bulletin of the Geological Society of America 95, 357–363.

Handin, J.W., Griggs, D., 1951. Deformation of Yule marble: Pt. II. Predicted fabric changes. Geological Society of America Bulletin 62, 863–886.

Heard, H.C., 1963. The effect of large changes in strain rate in the experimental deformation of the Yule marble. Journal of Geology 71, 162–195.

Hobbs, B.E., Means, W.D., Williams, P.F., 1976. An Outline of Structural Geology. John Wiley and Sons, New York.

Jaeger, J.C., Cook, N.G.W., 1979. Fundamentals of Rock Mechanics, 3rd ed, Chapman and Hall, London.

Kennedy, L.A., White, J.C., 2001. Low-temperature recrystallization in calcite: mechanisms and consequences. Geology 29, 1027–1030.

Mosar, J., 1988. Metamorphism transporte dans les Prealpes. Schweizerische Mineralogische and Petrographische Mitteilungen 68, 77–94.

Mosar, J., 1989. Deformation interne dans les Prealpes medianes (Suisse). Eclogae geologicae Helvetiae 82, 765–793.

Rowe, K.J., Rutter, E.H., 1990. Paleostress estimation using calcite twinning: experimental calibration and application to nature. Journal of Structural Geology 12, 1–17.

Rutter, E.H., 1976. The kinetics of rock deformation by pressure solution. Philosophical Transactions of the Royal Society of London A283, 203–219.

Schmid, S.M., 1982. Microfabric studies as indicators of deformation mechanisms and flow laws operative in mountain building. In: Hsu, K., (Ed.), Mountain Building Processes, Academic Press, London, pp. 95–110.

Schmid, S.M., Paterson, M.S., Boland, J.N., 1980. High temperature flow and dynamic recrystallization in Carrara Marble. Tectonophysics 65, 245–280.

Smart, K.J., Dunne, W.M., Krieg, R.D., 1997. Roof sequence response to emplacement of the Wills Mountain duplex: the roles of forethrusting and scales of deformation. Journal of Structural Geology 19, 1443–1459.

Spang, J.H., Groshong, R.H. Jr, 1981. Deformation mechanisms and strain history of a minor fold from the Appalachian Valley and Ridge Province. Tectonophysics 72, 323–342.

Spang, J.H., Oldershaw, A.E., Groshong, R.H. Jr, 1974. The nature of thin twin lamellae in calcite. EOS 55, 419.

Spraggins, S.A., Dunne, W.M., 2002. Deformation history of the Roanoke recess, Appalachians, USA. Journal of Structural Geology 24, 411–433.

Spry, A., 1969. Metamorphic Textures. Pergamon Press, Oxford.

Turner, F.J., 1953. Nature and dynamic interpretation of deformation lamellae in calcite of three marbles. American Journal of Science 251, 276–298.

Turner, F.J., Ch'ih, C.S., 1951. Deformation of Yule marble: Part III. Observed fabric changes due to deformation at 10,000 atmospheres confining pressure, room temperature, dry. GSA Bulletin 62, 887–906.

Xu, J., 1993. Strain analysis of Lower and Middle Paleozoic units in the Great Valley Province and its significance to the fold mechanics in the Massanutten Synclinorium, Virginia. M.Sc. thesis. Bowling Green State University, Bowling Green, Ohio, USA.

Xu, J., Onasch, C.M., Shen-tu, B., 1993. Regional strain variations and fold mechanics in the Massanutten Synclinorium, northwest Virginia. Geological Society of America Abstracts with Programs 25, A168.